Microchemostat—microbial continuous culture in a polymer-based, instrumented microbioreactor

Zhiyu Zhang,[a] Paolo Boccazzi,[b] Hyun-Goo Choi,[a] Gerardo Perozziello,[c] Anthony J. Sinskey[b] and Klavs F. Jensen*[a]

Received 5th January 2006, Accepted 4th April 2006
First published as an Advance Article on the web 20th April 2006
DOI: 10.1039/b518396k

In a chemostat, microbial cells reach a steady state condition at which cell biomass production, substrates and the product concentrations remain constant. These features make continuous culture a unique and powerful tool for biological and physiological research. We present a polymer-based microbioreactor system integrated with optical density (OD), pH, and dissolved oxygen (DO) real-time measurements for continuous cultivation of microbial cells. *Escherichia coli* (*E. coli*) cells are continuously cultured in a 150 μL, membrane-aerated, well-mixed microbioreactor fed by a pressure-driven flow of fresh medium through a microchannel. Chemotaxisial back growth of bacterial cells into the medium feed channel is prevented by local heating. Using poly(ethylene glycol) (PEG)-grafted poly(acrylic acid) (PAA) copolymer films, the inner surfaces of poly(methyl methacrylate) (PMMA) and poly(dimethylsiloxane) (PDMS) of the microbioreactor are modified to generate bio-inert surfaces resistant to non-specific protein adsorption and cell adhesion. The modified surfaces of microbioreactor effectively reduce wall growth of *E. coli* for a prolonged period of cultivation. Steady state conditions at different dilution rates are demonstrated and characterized by steady OD, pH, and DO levels.

1. Introduction

There is great interest in the development of new cell cultivation technologies for high-throughput screening and bioprocess development. Conventional microbial cell cultivation techniques use instrumented bench-scale stirred-tank bioreactors with typical volumes of between 0.5 and 10 liters, with control of temperature, pH, and dissolved oxygen (DO) levels. These systems yield valuable physiological and metabolic data, but they typically consume large amounts of supplies and are labor intensive. Simple laboratory-scale bioreactors with reduced working volumes, including microtiter plates, test tubes, and shake flasks, can easily be operated in parallel and with smaller volumes, but often lack integration of on-line sensors. Fermentation experiments using these bioreactors are mostly batch processes and information is often obtained only as end point measurements. Thus, there is a need for miniaturized, instrumented systems that allow rapid testing, process development, and optimization to be carried out in parallel fermentations.

Microbioreactor technology with integrated real-time measurements is a promising solution for high-throughput systems. Kumar *et al.*[1] review early developments in the field. In the microbioreactor by Maharbiz *et al.*,[2,3] microtiter plate wells are combined with silicon technology to realize 250 μL microbioreactor arrays with integrated optical density (OD) measurement and pH ion-selective field effect transistor (ISFET) sensors on a printed circuit board. Oxygen is generated and delivered by water hydrolysis. Compared with electrochemical sensors, optical sensors are non-invasive, reliable, and inexpensive, all of which is advantageous for high-throughput screening and for moving towards development of disposable microbioreactors. Rao and co-authors[4–7] pioneered optical sensors for continuous measurements of OD, pH, and DO in a 2 mL cuvette for microbial batch cultures. Similar optical sensors are used in miniature bubble column bioreactors,[8,9] which can be viewed as scaled-down versions of conventional bench-scale stirred-tank bioreactors. Optical monitoring was also implemented by Zanzotto *et al.*[10] in a 5 μL membrane-aerated microbioreactor. Recently, a system has been reported with 48 magnetically-mixed milliliter scale bioreactors, each with OD and pH real time measurements.[11–13] This system enables the automation of fed-batch operation and pH control. The above examples of miniaturization and parallelization of microbioreactors, as well as emerging commercial systems (*e.g.*, Cellstation, Fluorometrix Corp., MA, USA and SimCell, BioProcessors, MA, USA) demonstrate the potential for obtaining valuable growth kinetic data from microbioreactors and indicate the promise of high-throughput technologies for bioprocessing.

Most microbioreactors reported to date operate in batch and fed-batch modes. In batch and fed-batch cultures, the properties of microorganisms, such as size, composition, and functional characteristics, vary considerably during the growth of the culture. Steady state cell growth, in which cell biomass, substrates and product concentrations remain constant, can

[a]*Department of Chemical Engineering, Massachusetts Institute of Technology, 77 Massachusetts Ave. 66-566, Cambridge, MA 02139, USA. E-mail: kfjensen@mit.edu; Fax: +1 617 258 8224; Tel: +1 617 253 4589*
[b]*Department of Biology and Health Sciences and Technology, Massachusetts Institute of Technology, 77 Massachusetts Ave. 68-370A, Cambridge, MA, USA*
[c]*MIC-Department of Micro and Nanotechnology, Technical University of Denmark (DTU), DK-2800, Kgs. Lyngby, Denmark*

only be realized in continuous culture experiments. Continuous culture enables the control of the chemical environment, independent of growth rates (chemostat). Therefore, the cause/effect relationship can be determined along with kinetic parameters and yield coefficients.[14] These features make a chemostat a unique and powerful tool for biological and physiological research. Efforts at miniaturization in parallel operation of continuous bioreactors have been made as well. Gu *et al.*[15] used a miniature stirred-tank bioreactor with a working volume of 58 mL in a two-stage continuous culture experiment and further applied it in a multi-channel system.[16] Walther *et al.*[17–19] developed a 3 mL continuous bioreactor with integrated microelectronic sensors for biomass, pH, and temperature to investigate physiological and morphological properties of yeast cells in microgravity environments in a space lab. The microbioreactor was a self-sustained and controlled system: medium flow rate measured by a microsensor was controlled by a piezo-electric silicon membrane pump; pH was measured by an ISFET sensor[17] and controlled by coulometric generation of hydroxyl ions at a titanium electrode. Aeration was through gas-permeable cylindrical silicone tubes in the bioreactor, and mixing was realized by a magnetic stir bar.[18] Recently Balagaddé *et al.*[20] described a microchemostat reactor composed of poly-(dimethylsiloxane) (PDMS) peristaltic pumps and valves using soft lithography technology. In this reactor $\sim 10^4$ *E. coli* cells were cultured in 15 nL liquid segments; mixing with fresh medium was obtained by circulating flow in a microfluidic loop. Furthermore, a perfusion-type microfluidic device was used by Groisman *et al.*[21] by physically trapping cells in nL-volume chambers. Although cells were cultivated in a batch process in the absence of active mixing, ''chemostat'' state was claimed as determined by constant growth conditions observed with the expression of a fluorescent protein.[22]

In this paper we present a well-mixed, membrane-aerated microbioreactor that functions as a microchemostat. Optical sensors for OD, pH, and DO measurements are integrated in the microbioreactor and interfaced with a computer for on-line monitoring. A volume of 150 μL in the microbioreactor makes sampling possible for bioanalysis, such as HPLC or global gene expression analysis.[23] Local cooling of the sampling section is implemented for off-line sampling. Active mixing is obtained using a mini magnetic stir bar. The construction of the microbioreactor in layers of poly(methylmethacrylate) (PMMA) and PDMS is inexpensive and compatible with large-scale injection-molding and hot-embossing fabrication processes.

In addition to the fundamental requirements for batch microbioreactor,[24] including medium mixing, oxygenation and OD, pH, and DO on-line measurements, a microchemostat requires a dynamic balance of medium feeding and cell growth to avoid ''wash-out'' or overpopulation of cells in the microbioreactor. Additional challenges for realizing chemostat performance in microdevices include avoiding cell growth on the reactor walls and avoiding chemotaxis of bacteria into microfluidic channels. The prolonged time for culture in chemostats means that cell adhesion and wall growth on the surfaces of the bioreactor can become significant issues unless reactor surfaces are modified to provide resistance to non-specific cell adhesion. Cells growing on surfaces have different physiological characteristics from those growing in suspension,[25] and thus cell wall growth kinetics deviate from the chemostat model.[26] This problem is further accentuated by the high surface-to-volume ratio of micro-scale devices.[27] Unlike the microbioreactor by Balagaddé *et al.*,[20] in which a lysis buffer was used to clean reactor surfaces periodically, we employ a coating method using poly(ethylene glycol) (PEG)-grafted poly(acrylic acid) (PAA) copolymer films on PDMS and PMMA surfaces to effectively reduce *Escherichia coli* cell adhesion and cell wall-growth. Chemotaxis, the bias random walk of motile bacterial cells towards nutrients, presents another major challenge for implementing microchemostats. A single cell migrating back through the feed line to the medium reservoir would rapidly contaminate the medium and ruin the chemostat experiment. We address this issue by implementing a local heating area in the microbioreactor to prevent chemotaxis of *E. coli*.

2. Materials and methods

2.1. Reactor design and fabrication

The microbioreactor was fabricated from four PMMA layers and two PDMS layers (see Fig. 1). The microbioreactor chamber (diameter 10 mm, depth 2 mm, total volume of 150 μL) and three connecting channels (depth 250 μm, width 250 μm) were fabricated in three bottom PMMA layers (1 mm, 1.5 mm, and 0.5 mm in thickness, Goodfellow Corp., Devon, PA, USA) by using a computer-numerical-controlled (CNC) milling machine. The three layers were thermally bonded using a mechanical press (140 kPa, 145 °C for 90 min). A thin layer (100 μm) of spin-coated PDMS (the mixing ratio of silicone to curing agent was 10:1, Sylgard 184, Dow Corning Corp., Midland, MI, USA) covered the reactor chamber and served as the aeration membrane. PDMS was spin-coated at a speed of 1200 rpm for 25 s and then baked at 70 °C for 2 hours for curing. To facilitate device assembly and hermetical sealing, this PDMS layer was bonded with a 5 mm-thick PDMS gasket

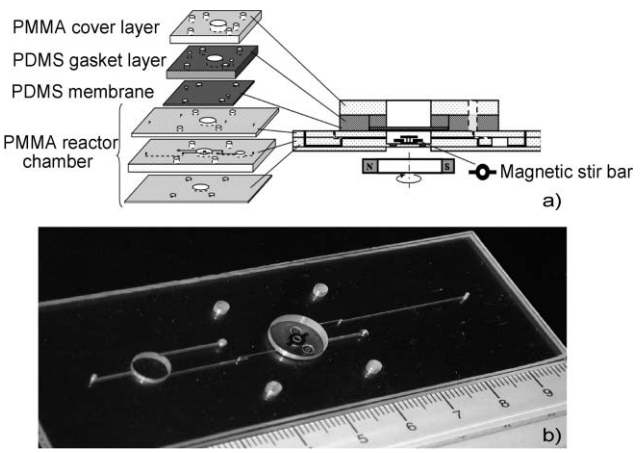

Fig. 1 (a) Schematic view of the longitudinal section of the microbioreactor utilized for continuous culture studies; (b) photograph of the empty PMMA chamber of the reactor (middle layer for reactor chamber) with the magnetic stir bar in the center.

layer. The PDMS layer was covered with an additional layer of stainless steel grid (B-PMX-062, Small Parts Inc., Miami, FL, USA) fixed by a home-made PDMS O-ring to provide a perforated membrane structure. A top PMMA layer was used to provide a rigid support in the mechanical assembly.

In the reactor chamber, two recesses (diameter 2 mm, depth 250 μm, 2.7 mm radial distance from the center) at the bottom of the bioreactor chamber accommodated pH and DO fluorescence lifetime sensors (DO sensor foil PSt3, and pH sensor solution HP2A, PreSens—Precision Sensing GmbH, Regensburg, Germany). A ringed magnetic stir bar with 6 mm arm length and 0.5 mm thickness (custom made by Engineered Concepts, Vestavia Hills, AL, USA) was used for active mixing. The rotation of the stir bar was fixed horizontally by a free-standing vertical post (height of 800 μm, diameter of 1.35 mm) and positioned vertically by a shallow shoulder (height of 200 μm, diameter of 2.2 mm) machined out of the bulk PMMA in the center of the reactor chamber. A piece of PMMA (250 μm thick and 3 mm diameter) was attached on top of the PMMA post by using acrylic solvent (Weld-On 4, IPS Corp., Gardena, CA, USA) to keep the magnetic stir bar in position (Fig. 1).

2.2. Fluidic connections and temperature control

Small connecting ports (660 μm in diameter) were drilled into the PMMA chip at two inlets (for inoculation and medium feeding, respectively) and two outlets (for exit to waste and sampling, respectively) of the microbioreactor. Stainless steel tubes (23 gauge, Small Parts, Inc., Miami Lakes, FL, USA) were fixed into these ports by epoxy and connected to polyethylene tubings (1/32″ outer diameter, Becton Dickinson, Franklin Lakes, NJ, USA). Fresh medium in a 10 mL glass syringe (Gastight, Becton Dickinson and Company) was pumped and fed to the microbioreactor by a syringe pump (PHD2000, Harvard Apparatus Inc., Holliston, MA, USA). The other side of the reactor was connected to a pressurized water reservoir (at 300 mm H_2O) that served as the effluent collector and also kept the reactor at a constant, positive pressure.

In the microchemostat, medium continuously flows through the microbioreactor, implying that motile bacteria, *e. g. E. coli*, can potentially migrate upstream into the nutrient reservoir. Two steps were taken to eliminate this chemotaxis behavior. First, the cross-section of the inlet microchannels were made small (250 μm × 250 μm). For typical flow rates (0.5 μL min^{-1} to 2 μL min^{-1}) the average linear flow rates (130 ∼ 500 μm s^{-1}) were significantly higher than the average migration speed of *E. coli* cells (20 ∼ 80 μm s^{-1}).[29] Second, we used a local heater (HP-127-1.0-0.8P, TE Technology, Inc., Traverse City, MI, USA) to raise the temperature of the feed line to ∼70 °C, which reversed the driving force for chemotaxis, since the cells have a tendency to adverse chemotaxis towards high temperature.[29,30] The high temperature zone provides an additional advantage of pasteurizing effect on cells. At the exit side of the chemostat, a peltier thermoelectrical cooler (HP-127-1.0-0.8P, TE Technology) reduced the local temperature of a 40 μL effluent reservoir (1.5 mm deep and 6 mm in diameter) to 4 °C to keep cells at low temperature and significantly reduce metabolic activity to facilitate off-line sampling for further analysis. Thin pieces of copper (1 mm in thickness) were placed underneath each section (heater, bioreactor, and cooler) within each region (Fig. 2) to ensure constant temperatue. The chamber temperature was measured by a thermocouple (TP-2444, TE Technology) and maintained at 37 °C by a temperature controller (TC-24-10, TE Technology). In order to evaluate the thermal design, the temperature distribution in the microbioreactor (Fig. 2) was simulated by the finite element method using Femlab® software (version 3.1, Comsol, Inc., Burlington, MA, USA).

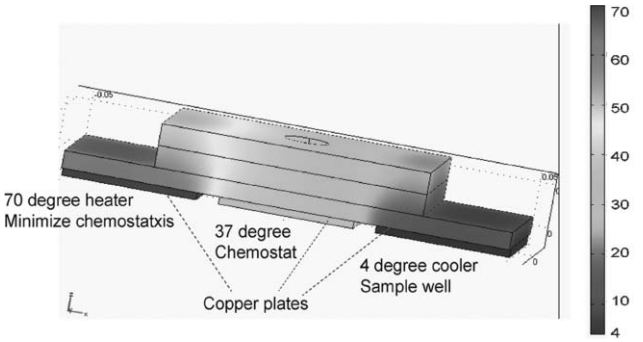

Fig. 2 Femlab simulation of temperature control and distribution in the microbioreactor. Microbioreactor chamber and microchannels are located at the bottom side of the device, thus temperature disturbances by native convection of air are not significant.

2.3. Optical measurement setup

The experimental set-up is shown in Fig. 3. DO, pH, and OD were measured by the optical sensing methods previously described in detail.[11] The microbioreactor was placed in an aluminium chamber maintained at 37 °C by flowing heated water through its base. An external magnetic stirrer (SP72725, Barnstead International, Dubuque, USA) was placed directly below the aluminium chamber which drove the movement of the ring-shape stir bar in the microbioreactor. Bifurcated optical fibers (custom-made by RoMack Fiber Optics, Williamsburg, VA, USA) led into the chamber from both the top and the bottom, and connected to LEDs and photo-detectors (PDA-55, Thorlabs, Newton, NJ, USA) to perform the optical measurements. Both dissolved oxygen and pH were measured using phase modulation lifetime fluorimetry. The DO and pH sensors, located in the recesses (*cf.* Fig. 1) at the bottom of the reactor chamber at a distance of 2.5 mm radial distance from the center, were excited with a blue–green LED (505 nm, NSPE590S, Nichia America Corporation, Mountville, PA, USA) and a blue LED (465 nm, NSPB500S, Nichia), respectively. Excitation bandpass filters (XF1016 and XF1014, Omega Optical, Inc., Brattleboro, VT, USA) and emission longpass filters (XF 3016 and XF 3018, Omega Optical) separated the respective excitation and emission signals and minimized their cross-excitation. OD data, closely related to biomass concentration in the microbioreactor, were obtained from an absorbance measurement using an orange LED (L600-10V, 600 nm, Epitex, Kyoto, Japan). The bifurcated branch (broken line in Fig. 3) yielded a reference signal to compensate for intensity fluctuations of the orange

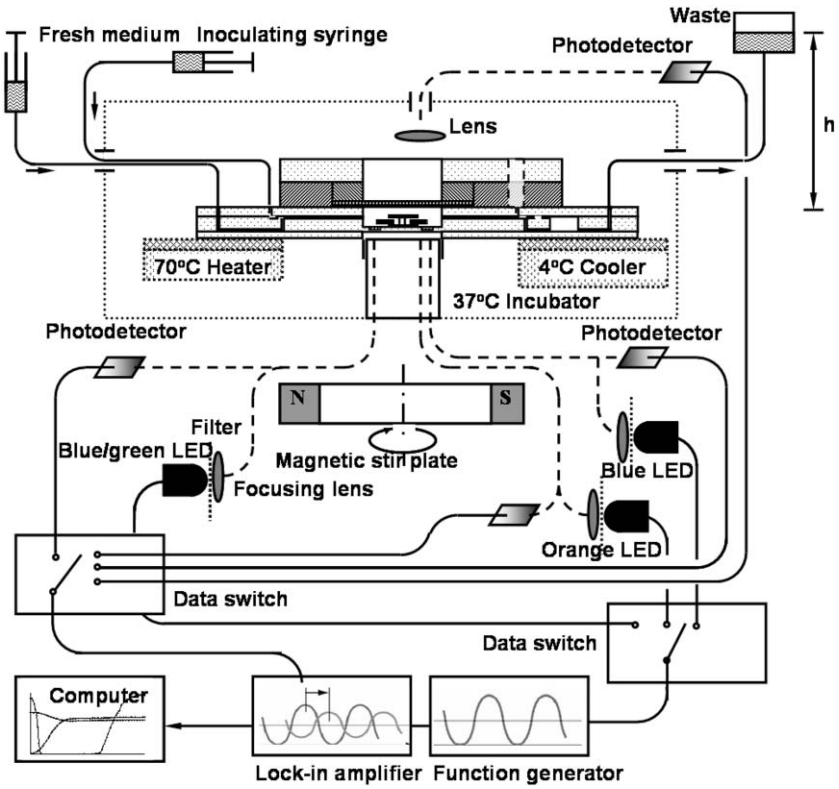

Fig. 3 Experimental setup for the microbioreactor (h = 30 cm). The microbioreactor is kept at 37 °C in an aluminium chamber. Three optical fibers carry different wavelengths of light to the bottom of the microbioreactor for OD, pH, and DO measurements, respectively. A computer collects and analyzes the transmitted or emitted light through photodetectors and a lock-in amplifier. Broken lines represent optical fibers.

LED. Data switches (7204, Electro Standard Laboratories, Cranston, RI, USA) multiplexed the output signal and the input signal of the function generator (33220A, Agilent Technologies, Palo Alto, CA, USA) and the lock-in amplifier (SR 830, Stanford Research Systems, Sunnyvale, CA, USA), respectively. All instruments were PC-controlled under LabVIEW® (National Instruments Corp., Austin, TX, USA), which enabled automated and real-time measurement of the parameters.

2.4. Surface modification procedures for PDMS and PMMA

We developed a coating method using poly(ethylene-*r*-propylene) copolymer–grafted poly(acrylic acid) (PAA) copolymer films (PAA-*g*-(PEG-*r*-PPG)) to generate bio-inert surfaces capable of effectively reducing non-specific cell adhesion on both PDMS and PMMA surfaces of the microbioreactor. PAA-*g*-(PEG-*r*-PPG) copolymer was synthesized using an amidation reaction to graft H_2N-(PEG-*r*-PPG)-OCH_3 (Jeffamine XTJ-234, Huntsman Co., Houston, TX, USA) chains to the carboxylic acid groups on the PAA (Sigma–Aldrich Co., St. Louis, MO, USA) backbone[31] with a grafting ratio of 50%. In a typical synthesis, a total of 23 g of the two polymers in the desired stoichiometric ratio was added to a reaction vessel. The mixture was heated to 180 °C for 2 h under a bubbling flow of N_2, which provided mixing, prevented oxidation, and expelled water produced by the condensation reaction. The product was cooled to room temperature and dissolved in deionized water to produce 33 wt% stock solution. Completion of the reaction was verified by the disappearance of free amine in a Ninhydrin test.[31,32]

The surface modification protocols, as shown in Fig. 4, started with O_2 plasma treatment for 30 s at 0.15 Torr in a Harrick Plasma Cleaner (PDC-32G, Harrick Scientific) for PDMS and reduction with 0.4 mol L^{-1} of $LiAlH_4$ in ether solution for 30 min for PMMA to generate hydroxyl groups on the surfaces. PDMS and PMMA layers were then immersed in a 1 wt% ethanolic solution of *N*-(6-aminohexyl) aminopropyl trimethoxysilane (AHPTS, Gelest, Inc. Morrisville, PA, USA) for 18 hours. After being removed from solution, rinsed with ethanol and dried under the stream of N_2, AHPTS-coated PDMS and PMMA layers were assembled into a microbioreactor. In the final step, the PAA-*g*-(PEG-*r*-PPG) copolymer films were assembled on the AHPTS-coated PDMS and PMMA surfaces by flowing an aqueous solution of the polymer (6 wt%, pH 7.4) through the microbioreactor, followed by rinsing with distilled water and drying under N_2.

2.5. Materials and methods for biological experiments

E. coli FB21591 (thiC::Tn5-pKD46, Kan^R), a derivative of *E. coli* K12, was obtained from the University of Wisconsin and used as a model organism. Two culture media were used for different experiments: Luria–Bertani (LB) rich medium containing 8 g L^{-1} glucose (Mallinckrodt, Hazelwood, MO, USA), 100 mg L^{-1} kanamycin (Sigma–Aldrich), and 0.1 mol L^{-1} 2-(*N*-morpholino)ethanesulfonic acid (MES) (Sigma–Aldrich), and MOPS minimal medium (Teknova, Inc., Hollister, CA,

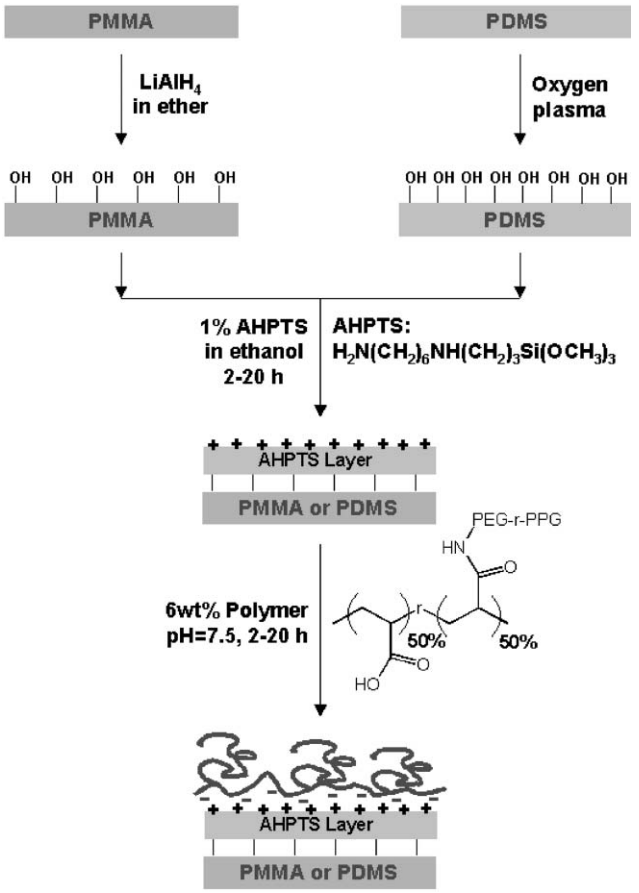

Fig. 4 Schematic illustration of surface modification of PMMA and PDMS using PAA-*g*-(PEG-*r*-PPG) copolymer films.

USA) containing 1 g L^{-1} glucose, 100 μmol L^{-1} thiamine (Sigma–Aldrich), and 100 mg L^{-1} kanamycin.

In each experiment, single colonies of *E. coli* FB21591 were transferred from LB plates containing 2% (w/v) agar and 100 μg L^{-1} of kanamycin, to 5 mL of sterile LB medium (containing 8 g L^{-1} glucose, 100 μg L^{-1} kanamycin, and 0.1 mol L^{-1} MES) in test tubes. These cultures were then incubated on a roller drum at 60 rpm and 37 °C. When the culture reached an $OD_{600\ nm}$ of 1 (Spectronic 20 Genesys, Spectronic Instruments, Leeds, UK), 1.5 mL of culture medium was transferred from test tubes to 30 mL of LB or MOPS medium in a 250 mL baffled shake flask. The shake flask was then incubated at 37 °C on a shaker operating at 150–220 rpm. The culture medium in the shake flask was used to inoculate the microbioreactor.

For microbioreactor experiments, DO, pH, and OD data were obtained on-line every 20 min after inoculation. Following each continuous culture experiment, the entire volume of the culture (~150 μL) was harvested and the final OD_{600} and pH values were measured. Calibration curves for OD readings were obtained by filling the microbioreactor with culture fluids of different biomass concentrations. The OD_{600} reading of the inoculum and the final OD_{600} reading were then used to calibrate real-time absorbance measurement. Since the optical absorbance of PDMS changes after being dipped in water,[33] the microbioreactor was filled with sterile water for more than 6 hours before each experiment to eliminate any potential changes in OD.

In order to test for any potential contamination of the medium, the medium in the feeding tubing was collected after each experiment and added to test tubes containing 5 mL of sterile LB medium. Turbidity measurements of the test tubes after incubation at 37 °C were used to detect growth in the feed medium. After compeletion of the culture, *E. coli* adhesion on the PMMA and PDMS surfaces in the microbioreactor chamber were captured by optical microscope (Nikon TE300). Safranin (Sigma–Aldrich) was used to stain *E. coli* cells on the PMMA surface.

3. Results and discussion

3.1. Steady state cell culture

A critical requirement for chemostat experiments is the ability to achieve and sustain steady state conditions. Fig. 5 shows an example of continuous culture experiments with *E. coli*, starting with an inoculum of concentrated and metabolically active cells in MOPS medium. After inoculation, cells utilized the carbon source, glucose, in the medium and consumed all available oxygen: thus, the DO level rapidly dropped to zero within a few hours. Correspondingly, the pH level of the culture broth decreased as a result of acetic acid by-product formation due to fermentation.[34] The OD in the microbioreactor increased at the beginning, indicating rapid cell growth, and decreased slowly due to limited glucose in the feeding stream and a slow feeding rate of 0.5 μL min^{-1}. The recovery of pH was significantly faster because little acid was produced after oxygen started to recover. After about 80 hours, DO, pH, and OD reached stable levels and steady state conditions in the microchemostat were established.

The net increase rate of bacterial biomass in suspension X is given by the simple mass balance:[35]

$$\frac{dX}{dt} = \mu X - DX \quad (1)$$

where μ is the specific growth rate and D is the dilution rate. At steady state the growth rate equals the dilution rate:

$$\mu = D = \frac{F}{V} \quad (2)$$

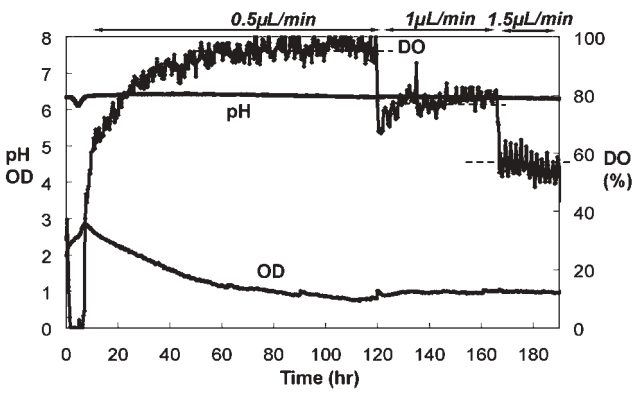

Fig. 5 Steady states in *E. coli* microchemostats at medium feeding rates of 0.5 μL min^{-1}, 1 μL min^{-1}, and 1.5 μL min^{-1}, respectively.

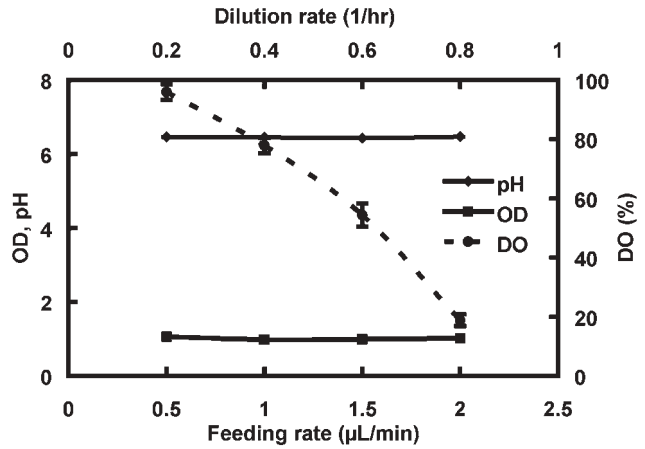

Fig. 6 Steady state conditions of *E. coli* culture in the microchemostat operating at different dilution rates.

With a medium feeding rate F of 1 μL min^{-1} and a reactor volume V of 150 μL, the specific cell growth rate μ, which equals the dilution rate D, was 0.4 h^{-1}. This relatively low growth rate was characterized by an OD level as high as ~81%, and the steady state was maintained for ~8 turnover times. Correspondingly, the OD_{600} level was ~1.05 and the pH level was 6.5.

In order to demonstrate that different steady states can be established by varying the dilution rate, the medium feed rate was increased sequentially from 0.5 μL min^{-1} to 1 μL min^{-1} and to 1.5 μL min^{-1}. Steady state conditions were maintained for at least 8 turnovers at each dilution rate. The observed steady DO levels were 94%, 77%, and 56%, respectively (Figs. 5 and 6). Lower DO levels at higher dilution rates are direct indications of faster growth and metabolism rates. Aerobic metabolism in the microchemostat resulted in a relatively stable pH level in the culture medium at different dilution rates due to sufficient oxidative catabolism and pH buffering from phosphates in the MOPS medium. The measurement for biomass concentration, OD_{600} level, also remained at a stable level of ~1 (biomass concentration of ~0.46 g cell dry weight L^{-1}), despite the changes of different dilution rates; this is consistent with the bioprocess stoichiometry observed in conventional bioreactors when glucose was used as the sole carbon and energy source for *E. coli* aerobic cultivation.[36,37]

3.2. Inhibition of back growth and wall growth of *E. coli*

Liquid medium upstream of the heated zone was incubated in fresh LB medium, and no cell growth was observed. In contrast, cells were present upstream of the unheated feeding channel. With the implementation of local heating of the medium feeding channel, chemotaxis and back growth of *E. coli* cells were effectively eliminated.

The extent of cell wall growth in the microbioreactor was also investigated. Fig. 7 shows the comparison of unmodifed and PAA-*g*-(PEG-*r*-PPG)-modified PDMS and PMMA surfaces of the microbioreactor after *E. coli* chemostat cultures. After a prolonged period (7 days) of cell culture, typical surface densities of *E. coli* on the unmodified PMMA and PDMS surfaces were estimated as 4.6×10^6 cells cm^{-2} and 2.8×10^6 cells cm^{-2}, respectively. On the other hand, the PAA-*g*-(PEG-*r*-PPG)-modified PMMA and PDMS surfaces exhibited a large reduction in *E. coli* adhesion by 92% (3.9×10^5 cells cm^{-2}) and 93% (2×10^5 cells cm^{-2}), respectively, relative to the unmodified PMMA and PDMS surfaces. By implementing the PAA-*g*-(PEG-*r*-PPG)-modified PDMS and PMMA surfaces into the microbioreactor, adhesion and wall growth of *E. coli* in the microbioreactor were effectively

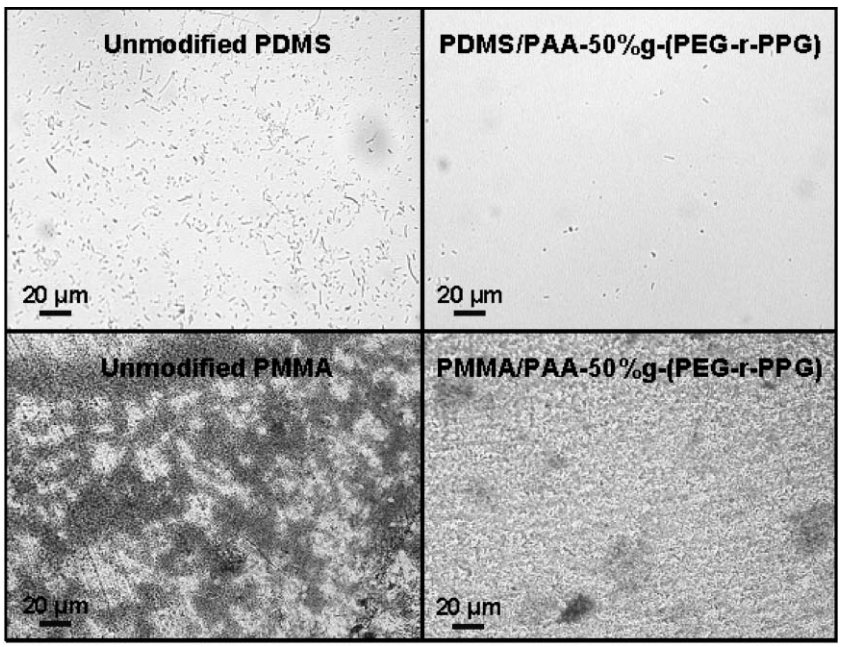

Fig. 7 Comparison of *E.coli* adhesion and wall growth of *E.coli* cells on PDMS and PMMA surfaces after continuous culture for 7 days in the microbioreactor. Cell adhesion on PAA-*g*-(PEG-*r*-PPG)-modified PDMS and PMMA surfaces were significantly reduced by 93% and 92%, respectively, relative to the unmodified surfaces.

reduced. As an estimate, the number ratio of wall attached cells over suspension cells is ~11% for unmodified microbioreactor and ~0.8% for PAA-*g*-(PEG-*r*-PPG) copolymer films-coated microbioreactor.

The effects of cell wall growth on bioprocess kinetics in the microbioreactor were further investigated by wash-out experiments, as summarized in Fig. 8. As a result of a sudden increment in medium feeding rate, most suspension cells were washed out of the microbioreactor and OD_{600} in the microbioreactor decreased dramatically in a short period of time (less than 20 min, Fig. 8). However, few attached bacterial cells were washed out by the high medium flow rate; instead these cells were surrounded by large amount of fresh medium and started to reproduce at the maximum growth rate. The resulting rapid recovery in growth was characterized by steady increases in absorption and decreases in DO (Fig. 8). This behavior is consistent with reported phenomena[38] and kinetic models[39] that incorporate wall growth into the conventional well-mixed continuous stirred tank reactor (CSTR) model. The minimum OD_{600} value observed in the wash-out experiment can be used to characterize the extent of cell wall growth. A comparison of Fig. 8(a) and 8(b) revealed that significantly less wall growth of *E. coli* is observed in the microbioreactor modified with PAA-*g*-(PEG-*r*-PPG) copolymer films than in the unmodified microbioreactor, very consistent with the cell count data (Fig. 7). In the microchemostat with modified reactor surfaces, the deviation from the expected behavior was much less significant, indicating that the employed method for surface modification is sufficiently effective to avoid the effects of wall growth.

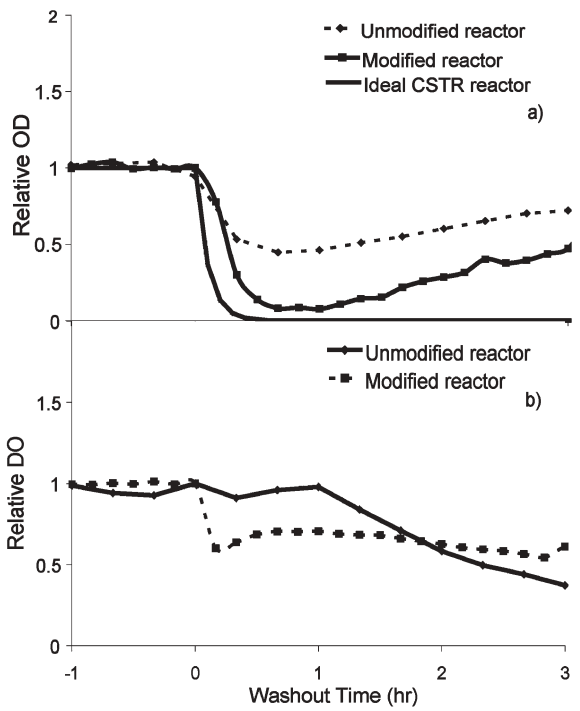

Fig. 8 Cell wash-out experiments in microchemostat. Wash-out experiments started with an increment of the medium feeding rate to 25 μL min^{-1} (turnover time of 12 min), which was significantly faster than the maximum reproduction rate of *E. coli* cells (doubling time of 23–27 mins). (a) Comparison of OD after wash-out. Steady OD levels before wash-out in unmodified and modified reactors are 1.00 and 1.01, respectively. (b) Comparison of DO after wash-out. Steady DO levels before wash-out in unmodified and modified reactors are 18% and 82%, respectively.

4. Conclusions

We have designed and fabricated a 150 μL membrane-aerated and actively mixed microbioreactor with multi-layers of PMMA and PDMS for continuous culture of microbial cells. PMMA and PDMS are chosen as structural materials for the bioreactor, for their good optical transparency to visible light, biocompatibility and chemical stability, as well as their potential for mass production. The latter characteristics would allow the microbioreactor to be disposable. Optical sensors for real time, *in situ* measurements of OD, pH, and DO are integrated into the microbioreactor.

With the combination of single-phase, pressure-driven medium feed at slow flow rates, local temperature control in the microbioreactor device, as well as the formation of a PEG-grafted PAA copolymer films on both PMMA and PDMS surfaces, a steady state of *E. coli* culture is obtained and sustained in the microchemostat with glucose as the only limiting substrate for growth. Bacterial chemotaxis and back growth are effectively inhibited by local heating in the medium feeding channel. Wall growth of bacterial cells in the microbioreactor is significantly reduced by the cell-resistant surfaces coated with PEG-grafted PAA copolymer films, even after a prolonged period of time cell cultivation. As a result, cell growth in microchemostats is dominated by the suspended cells in the microbioreactor chamber.

Time profiles of OD, pH, and DO measurements demonstrate the dynamic balance between cell growth rates and medium feed rates at steady state conditions. Kinetics and cell growth stoichoimetry in the microchemostat are consistent with phenomena reported in conventional stirred-tank bioreactors, but with 10^3 times smaller volumes than those of typical bench systems. The ability to control the growth rate of *E. coli* by varying the medium feed rate implies that the microchemostat could be an effective tool in investigations of cell physiology and metabolic rates. Integration of the microbioreactors into a multiplexed format will enable parallel operations, as previously demonstrated for micro batch reactors,[40] which should offer a platform towards high throughput systems to be used in rapid screening and analysis of biochemical processes.

Acknowledgements

The authors gratefully acknowledge funding from the DuPont–MIT Alliance (DMA).

References

1 S. Kumar, C. Wittmann and E. Heinzle, *Biotechnol. Lett.*, 2004, **26**, 1–10.
2 M. M. Maharbiz, W. J. Holtz, S. Sharifzadeh, J. D. Keasling and R. T. Howe, *J. Microelectromech. Syst.*, 2003, **12**, 590–599.
3 M. M. Maharbiz, W. J. Holtz, R. T. Howe and J. D. Keasling, *Biotechnol. Bioeng.*, 2004, **85**, 376–381.

4 Y. Kostov, P. Harms, L. Randers-Eichhorn and G. Rao, *Biotechnol. Bioeng.*, 2001, **72**, 346–352.
5 P. Harms, Y. Kostov and G. Rao, *Curr. Opin. Biotechnol.*, 2002, **13**, 124–127.
6 H. R. Kermis, Y. Kostov and G. Rao, *Analyst*, 2003, **128**, 1181–1186.
7 P. Harms, Y. Kostov, J. A. French, M. Soliman, M. Anjanappa, A. Ram and G. Rao, *Biotechnol. Bioeng.*, 2006, **93**, 6–13.
8 S. R. Lamping, H. Zhang, B. Allen and P. A. Shamlou, *Chem. Eng. Sci.*, 2003, **58**, 747–758.
9 S. D. Doig, A. Diep and F. Baganz, *Biochem. Eng. J.*, 2005, **23**, 97–105.
10 A. Zanzotto, N. Szita, P. Boccazzi, P. Lessard, A. J. Sinskey and K. F. Jensen, *Biotechnol. Bioeng.*, 2004, **85**, 376–381.
11 R. Puskeiler, K. Kaufmann and D. Weuster-Botz, *Biotechnol. Bioeng.*, 2005, **89**, 512–523.
12 R. Puskeiler, A. Kusterer, G. T. John and D. Weuster-Botz, *Biotechnol. Appl. Biochem.*, 2005, **42**, 227–235.
13 D. Weuster-Botz, R. Puskeiler, A. Kusterer, K. Kaufmann, G. T. John and M. Arnold, *Bioprocess Biosyst. Eng.*, 2005, in the press.
14 A. Akgün, B. Maier, D. Preis, B. Roth, R. Klingelhöfer and J. Büchs, *Biotechnol. Prog.*, 2004, **20**, 1718–1724.
15 M. B. Gu, G. C. Gil and J. H. Kim, *Biosens. Bioelectron.*, 1999, **14**, 355–361.
16 M. B. Gu and G. C. Gil, *Biosens. Bioelectron.*, 2001, **16**, 661–666.
17 I. Walther, B. H. van der Schoot, M. Boillat and A. Cogoli, *Chimia*, 1999, **53**, 75–80.
18 I. Walther, B. H. van der Schoot, M. Boillat and A. Cogoli, *Enzyme Microb. Technol.*, 2000, **27**, 778–783.
19 I. Walther, B. Bechler, O. Müller, E. Hunzinger and A. Cogoli, *J. Bacteriol.*, 1996, **47**, 113–127.
20 F. K. Balagaddé, L. You, C. L. Hansen, F. H. Arnold and S. R. Quake, *Science*, 2005, **309**, 137–140.
21 A. Groisman, C. Lobo, H. Cho, J. K. Campbell, Y. S. Dufour, A. M. Stevens and A. Levchenko, *Nat. Methods*, 2005, **2**, 685–689.
22 N. Q. Balaban, *Nat. Methods*, 2005, **2**, 648–649.
23 M. E. Lidstrom and D. R. Meldrum, *Nat. Rev. Microbiol.*, 2003, **1**, 158–164.
24 D. E. Dykhuizen and D. L. Hartl, *Microbiol. Rev.*, 1983, **47**, 150–168.
25 S. S. Pilyugin and P. Waltman, *SIAM J. Appl. Math.*, 1999, **59**, 1552–1572.
26 H. H. Topiwala and G. Hamer, *Biotechnol. Bioeng.*, 1971, **13**, 919–922.
27 P. Boccazzi, A. Zanzotto, N. Szita, S. Bhattacharya, K. F. Jensen and A. J. Sinskey, *Appl. Microbiol. Biotechnol.*, 2005, **68**, 518–532.
28 T. D. Brook, M. T. Madigan, J. M. Martinko and J. Parker, *Biology of Microorganisms*, Prentice Hall, Englewood Cliffs, NJ, 1994, p. 68.
29 K. Maeda, Y. Imae, J. Shioi and F. Oosawa, *J. Bacteriol.*, 1976, **127**, 1039–1046.
30 J. Adler, *Sci. Am.*, 1976, **234**, 40–47.
31 G. D. Moeser, K. A. Roach, W. H. Green, P. E. Laibinis and T. A. Hatton, *Ind. Eng. Chem. Res.*, 2002, **41**, 4739–4749.
32 E. Curotto and F. Aros, *Anal. Biochem.*, 1993, **211**, 240–241.
33 W.-J. Chang, D. Akin, M. Sedlak, M. R. Ladisch and R. Bashir, *Biomed. Microdevices*, 2003, **5**, 281–290.
34 K. Han, H. C. Lim and J. Hong, *Biotechnol. Bioeng.*, 1993, **39**, 663–671.
35 D. Herbert, R. Elsworth and R. C. Telling, *J. Gen. Microbiol.*, 1956, **14**, 601–622.
36 R. J. Harvey, *J. Bacteriol.*, 1970, **104**, 698–706.
37 M. L. Shuler and F. Kargi, *Bioprocess Engineering: Basic Concepts*, 2001, Prentice Hall.
38 D. H. Larsen and R. L. Dimmick, *J. Bacteriol.*, 1964, **88**, 1380–1387.
39 A. Moser, *Bioprocess Technology: Kinetics & Reactors*, 1988, Springer.
40 N. Szita, P. Boccazzi, Z. Zhang, P. Boyle, A. J. Sinskey and K. F. Jensen, *Lab Chip*, 2005, **5**, 819–826.